Shabnam Mirizadeh[1]
Saleh Al Arni[2]
Mahmoud Elwaheidi[3]
Alsamani A. M. Salih[2,4]
Attilio Converti[1]
Alessandro Alberto Casazza[1,*]

Adsorption of Tetracycline and Ciprofloxacin from Aqueous Solution on Raw Date Palm Waste

Supporting Information available online

Raw date palm waste was investigated as an adsorbent to remove tetracycline (TC) and ciprofloxacin (CIP) from water. Influence of pH, biosorbent dose, starting antibiotic concentration, contact time, temperature, and concentrations of different salts were examined. The pseudo-second-order model provided the best fit to the experimental data, while Langmuir and Dubinin-Radushkevich isotherms were found to be the most suitable for TC and CIP adsorption at equilibrium, respectively. Thermodynamic parameters indicated that the process is spontaneous and endothermic. These findings suggest that this waste could be a cost-effective and eco-friendly adsorbent to remove antibiotics from wastewater.

Keywords: Adsorption, Ciprofloxacin, Date palm waste, Tetracycline

Received: April 06, 2023; *revised:* June 03, 2023; *accepted:* June 06, 2023

DOI: 10.1002/ceat.202300193

1 Introduction

Global population, industrialization, and urbanization have resulted in an escalation of pollution, particularly in developing countries [1]. Throughout the world, there are growing concerns regarding the excessive use of antibiotics and their release into the environment [2]. Even though concentrations are much lower than therapeutic doses, these chemicals are constantly released in the environment due to the lack of restrictions on their discharge; therefore, their levels remain relatively constant, posing significant toxicological concerns for aquatic ecosystems and human health [3,4]. Accordingly, it is necessary to act on removing them from water bodies.

Conventional treatment processes proved to be ineffective when the antibiotic concentration in water is between 10 and 100 mg L^{-1} [5]. Methods such as filtration, coagulation, biological treatment, or advanced oxidation processes have been used, but each of them has their own limitations including high cost, heavy equipment, and tricky handling [6–8], thus leading to a higher demand for environmentally friendly, energy-efficient, and economically sustainable technologies.

Among treatments, adsorption is preferred since it is simple, easily manageable, and does not produce sludge or other pollution [9–11]. The US Environmental Protection Agency has endorsed activated carbon as a viable adsorbent to remove organic pollutants owing to its high porosity and surface area [12]. However, its use is not feasible on a large scale because its production is expensive and its regeneration impractical chemically and thermally, resulting in excess effluent and considerable adsorbent loss [13]. Thus, a lot of studies have been performed in recent years to prepare and develop low-cost alternatives. Among them, agricultural wastes and plant residues can be a good option because of easy access [14–16].

Date palm (DP) fiber and petiole are lignocellulosic materials containing approximately 40–50 % cellulose, 20–35 % hemicellulose, and 15–35 % lignin [17]. Lignin, which is the most valuable part of DP waste from the adsorption viewpoint, has a complex chemical structure consisting of three-dimensional units of phenylpropane linked through C–C and C–O–C bonds. This structure is responsible for a high percentage of carbon (62 wt %) and a low percentage of oxygen (32 wt %) in its elemental composition, which make lignocellulosic materials especially suitable as adsorbents.

DP-based adsorbents can effectively remove heavy metals and other pollutants even in small amounts [14]. For instance, it was reported for DP fiber a Pb^{2+} maximum adsorption

---

[1] Dr. Shabnam Mirizadeh https://orcid.org/0000-0002-2690-6279,
Prof. Dr. Attilio Converti https://orcid.org/0000-0003-2488-6080,
Prof. Dr. Alessandro Alberto Casazza
https://orcid.org/0000-0001-6851-6386
(alessandro.casazza@unige.it)
University of Genoa, Department of Civil, Chemical and Environmental Engineering, via Opera Pia 15, 16145 Genoa, Italy.

[2] Prof. Dr. Saleh Al Arni https://orcid.org/0000-0002-4592-8254,
Prof. Dr. Alsamani A. M. Salih
https://orcid.org/0000-0001-9007-3980
University of Ha'il, Department of Chemical Engineering, College of Engineering, P.O. Box 2440, Ha'il, 81441, Saudi Arabia.

[3] Prof. Dr. Mahmoud Elwaheidi
https://orcid.org/0000-0003-4863-3184
Geology and Geophysics Department, King Saud University, P.O. Box 2455, Riyadh, 11451, Saudi Arabia.

[4] Prof. Dr. Alsamani A. M. Salih
Al Neelain University, Department of Chemical Engineering, Faculty of Engineering, Khartoum, Sudan.

capacity (q_m)[1] (18.6–30.0 mg g^{-1}) comparable to that reported for hazelnut shells (28.18 mg g^{-1}) [18], a Cu^{2+} q_m (39.6 mg g^{-1}) [19] close to the one of rice husk (31.8 mg g^{-1}) [20] and an As(V) q_m (25.0 mg g^{-1}) remarkably higher than that of tea fungal biomass (4.95 mg g^{-1}) [21]. As for other pollutant classes, q_m values of 4.35 mg g^{-1} [22] and 58.14 mg g^{-1} [23] were reported for phosphate and methylene blue dye, respectively.

Despite the significance of antibiotic removal from water, there is a lack of studies on this issue. Therefore, this study aimed to address this gap by investigating the potential of raw DP as an adsorbent. To achieve this aim, it was focused on raw DP fiber use to adsorb tetracycline (TC) and ciprofloxacin (CIP) from aqueous solution, since these compounds are present in water effluents in concentration ranges of 0.06 µg L^{-1}–12.36 mg L^{-1} [24] and 0.248 µg L^{-1}–50 mg L^{-1} [25,26], respectively. The factors mostly influencing biosorption, i.e., pH, biosorbent dose, starting antibiotic concentration, contact time, temperature, and presence of different salts, were tested to determine the adsorption properties under different conditions, while kinetic and isotherm models and thermodynamic parameters were used to explore the sorption mechanism.

2 Materials and Methods

2.1 Adsorbent Preparation

DP waste was collected in a region of Saudi Arabia. Pieces (1 mm in length) were rinsed several times with distilled water to remove water-soluble materials and dirt particles, dried for one night in an air oven at 105 °C, left to cool at room temperature (20 ± 1 °C) and crushed. The powder was then sieved to obtain uniform size particles.

2.2 Adsorbent Characterization

DP surface morphology, before and after adsorption, was examined with a scanning electron microscope (SEM) (Hitachi 2500, Tokyo, Japan). Infrared spectra were obtained using a Fourier transform infrared (FTIR) spectroscope (Thermo Scientific, Madison, WA, USA). The immersion method was used to determine the zero point of charge (pH$_{zpc}$) [27].

2.3 Batch Adsorption Experiments

TC and CIP removal was investigated by changing the starting pH (3–11), biosorbent dose (0.25–5 g L^{-1}), contact time (0–120 min), and starting antibiotic concentration (10–150 mg L^{-1}). For this purpose, 50-mL flasks were filled with 30 mL of TC or CIP solution at different concentrations and shaken in an incubator at room temperature. Also, the influence of background electrolytes (up to 0.5 M NaCl or up to 0.1 M KCl or CaCl$_2$) was studied. Aliquots collected after various times were filtered through 0.45-µm pore diameter filters. Experiments were performed under optimized condition for each variable ensuring the highest adsorption capacity. NaOH or HCl was used to adjust the solution pH. Concentrations of antibiotics before and after adsorption were measured through calibration curves of absorbance readings in a UV-vis spectrophotometer (Lambda 25, PerkinElmer, Milan, Italy) of TC and CIP standard solutions at their maximum absorbance wavelengths (360 and 278 nm, respectively) versus concentration.

The antibiotics removal efficiency (Y, %) and equilibrium adsorption capacity (q_e, mg g^{-1}) were defined as:

$$Y(\%) = \left(\frac{C_0 - C_e}{C_0}\right) \times 100 \tag{1}$$

$$q_e = \frac{(C_0 - C_e)V}{m} \tag{2}$$

where C_0 and C_e (mg L^{-1}) are the antibiotics concentrations at the start and equilibrium, respectively, m is the weight of dried biosorbent (g), and V is the solution volume (L). Duplicate experiments were performed, and results were presented as mean values plus standard deviations.

2.4 Adsorption Isotherms, Kinetics, and Thermodynamics

Equations of the kinetic and isotherm models as well as the thermodynamic parameters are given in the Supporting Information (Sect. S1).

3 Results and Discussion

After its characterization by SEM and FTIR before and after TC and CIP adsorption (Supporting Information, Sect. S2) and determination of its pH$_{zpc}$ (6.8) (Fig. S3 of the Supporting Information), DP fiber was tested as an adsorbent under varying conditions.

3.1 Effect of Initial pH

Since the initial solution pH influences the degree of adsorbate ionization, hydrophilicity, solubility, and adsorbent surface charge [28,29], its effect on biosorption was explored by varying it from 3 to 11 at a constant TC or CIP concentration of 50 mg L^{-1}.

The adsorption capacity (q) towards TC (a) grew when the pH was increased from 3 to 5, (b) remained almost constant at pH 5–8, (c) reached the highest value (16.15 mg g^{-1}) at pH 10, but (d) fell at pH 11 (Fig. 1a). This behavior can be justified by the fact that TC exists as a cation at pH < 3.3 and zwitterion or anion at pH 3.3–9.7 and becomes completely negatively charged at pH > 9.7 [30]. In particular, acidic conditions impair TC adsorption due to the repulsive forces between its molecules and DP surface, both positively charged. As the pH was raised, the number of cationic species decreased, TC molecules were mainly present as zwitterions, and TC ion exchange occurred on DP surface. Interestingly, TC adsorption was enhanced by raising the solution pH until pH 10, at which DP

---

[1] List of symbols at the end of the paper.

surface was negatively charged, and TC molecules existed mainly as anions. The strong interaction between the bulk system on DP surface and benzene rings of TC molecules can be attributed to hydrogen bonds, van der Waals forces, or even π-π interactions, similar to what was reported for other adsorbents [31–33]. However, as the pH increased further to 10, the strong repulsion resulted in a q reduction.

The trend of CIP adsorption was opposite to that of TC (Fig. 1b). At low pH, a q value of approximately 30 mg g^{-1} was obtained, which suggests conditions under which both adsorbent surface and adsorbate were positively charged. Increasing pH from 4 to 7, q was reduced and kept almost constant in the 7–11 range. Since CIP molecules exist as cations at pH < 5.9, zwitterions at 5.9–8.9, and anions at pH > 8.9 [34], at low pH adsorption was controlled by non-electrostatic interactions, such as hydrophobic or π-π forces, while in the 6–9 pH range electrostatic interactions between positively charged amine group present in CIP zwitterion and negatively charged adsorbent surface may have been responsible for effective adsorption. At pH > 9, adsorption was still significant likely due to hydrogen bonds between CIP and C–O functional groups on surface.

On the basis of these considerations, a schematic representation of possible interactions between DP's surface functional groups and antibiotics can be proposed (Fig. 2).

3.2 Effects of Initial Concentration and Adsorption Time

There is a large variability in the concentration of wastewater discharged by pharmaceutical industries; therefore, investigating the impact of initial concentration of targeted antibiotics (C_0) is paramount. Variations in q and removal efficiency (Y) towards TC and CIP along the time at different C_0 are depicted in Fig. 3.

As for TC, q reached a maximum value of 24.5 mg g^{-1} when C_0 was raised from 10 to 80 mg L^{-1}, but remained almost constant at higher concentrations (Fig. 3a), while Y showed an opposite trend reaching a maximum value (54.8 %) at the lowest C_0 (Fig. 3b). As for CIP, q progressively increased up to 32 mg g^{-1} at 100 mg L^{-1}, beyond which it did not show any significant change (Fig. 3c), while a maximum Y value (58.75 %) was found at C_0 of 30 mg L^{-1} (Fig. 3d).

Y and q of either antibiotic grew quickly during the first 60 min and then decreased gradually, reaching equilibrium after 120 and 90 min for TC and CIP, respectively. The starting increase in q can be associated with the presence of a stronger driving force at high concentration, coupled with the availability of an adequate number of free binding sites on surface. Conversely, its subsequent reduction can be attributed to progressive active site saturation. Similar trends were previously reported for other sorbents [35–37].

3.3 Effect of Biosorbent Dose

To minimize biosorbent quantity and maximize q, the DP dosage was varied from 0.25 to 5 g L^{-1}

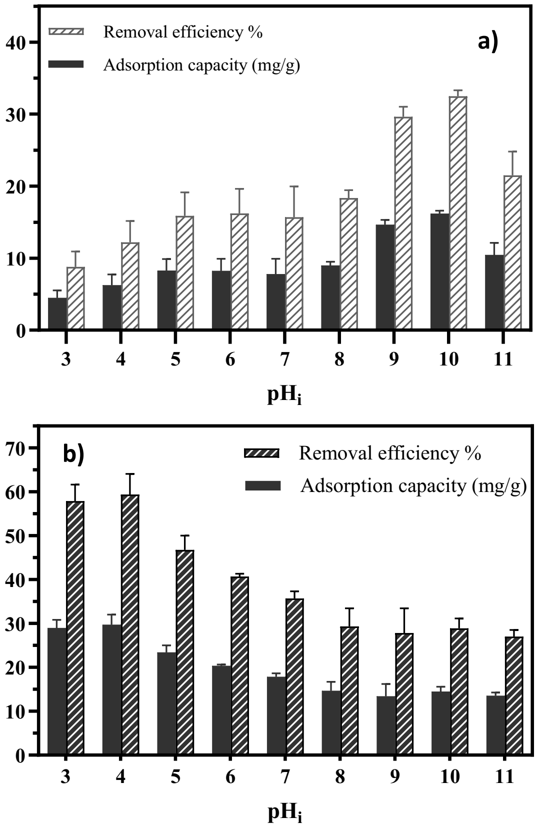

Figure 1. Effect of initial pH (pH$_i$) on tetracycline (TC) (a) and ciprofloxacin (CIP) (b) adsorption onto date palm (DP) fiber. Initial TC and CIP concentration: 50 mg L^{-1}, DP fiber dose: 1 g L^{-1}, temperature: 298 K, adsorption time: 3 h.

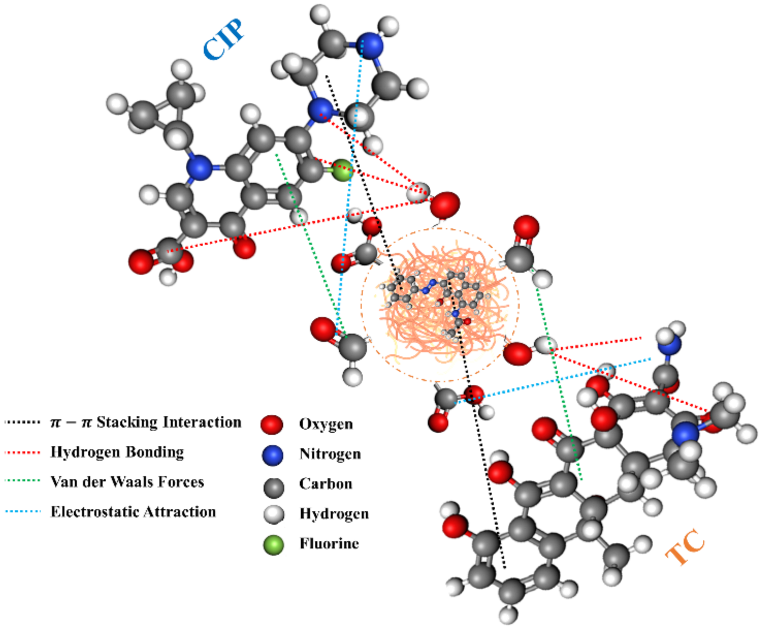

Figure 2. Schematic representation of possible interactions between DP's surface functional groups and antibiotics.

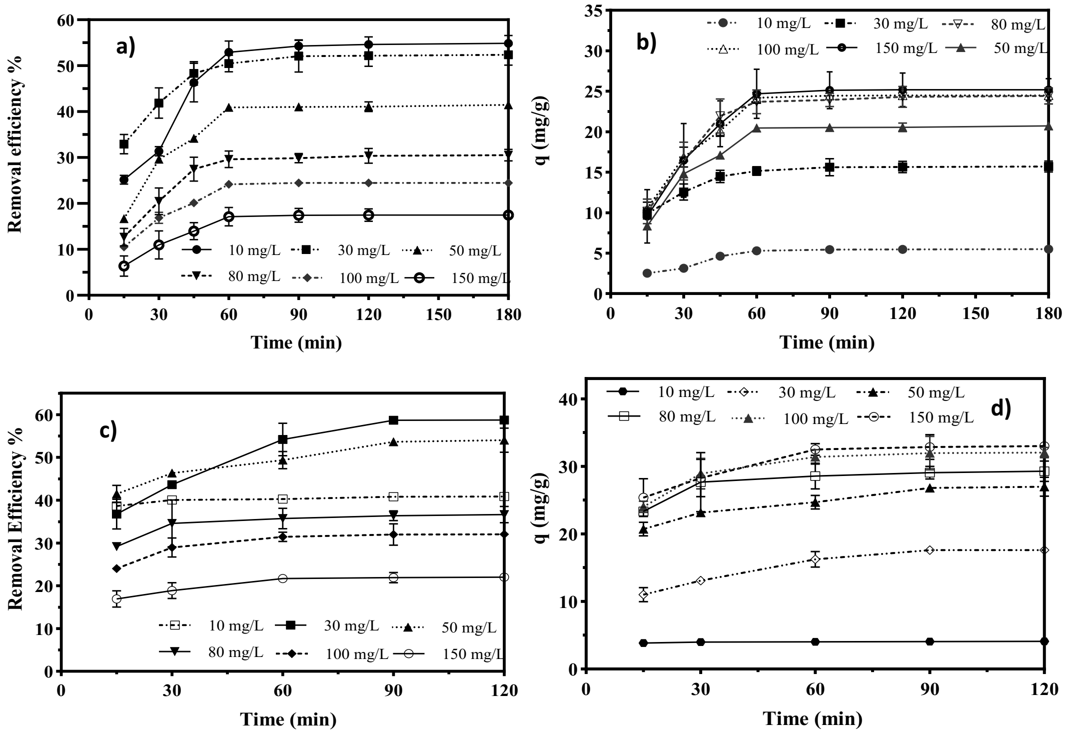

Figure 3. Effect of starting antibiotic concentration on the adsorption of tetracycline (TC) (a, b) and ciprofloxacin (CIP) (c, d) onto date palm fiber. q: adsorption capacity, DP fiber dosage: 1 g L^{-1}, temperature: 298 K.

(Fig. 4). Due to the increased active site number, Y towards TC and CIP grew rapidly and achieved 84.77 and 66.7 % at 5 g L^{-1}, respectively. However, q showed a decreasing trend at dosage > 1 g L^{-1} for TC and 0.5 g L^{-1} for CIP, likely due to an excessive rise in the number of unoccupied binding sites. Maximum values of q for TC and CIP were 23.24 and 44.78 mg g^{-1}, respectively. Therefore, equilibrium and kinetic studies were performed using these dosages.

3.4 Effect of Background Electrolytes

To assess the impact of salts on antibiotic adsorption, tests at varying NaCl, $CaCl_2$, and KCl concentrations were conducted (Fig. 5), considering the occurrence of Na^+, Ca^{2+}, and K^+ ions in both natural water and wastewater. A decrease in TC and CIP q was observed as NaCl concentration was increased from 0.0 to 0.5 M or that of the other two electrolytes up to 0.1 M, confirming the involvement of electrostatic interactions in the adsorption. Such a decrease may have been due to salts' competition with antibiotics for adsorption sites, leading to a reduction of adsorbent affinity [38, 39].

3.5 Adsorption Kinetics, Isotherms, and Thermodynamics

Fig. 6 illustrates the fitting of kinetic equations to the results of TC and CIP adsorption onto DP, while Tab. 1 lists the values of their kinetic parameters. Higher determination coefficient (R^2)

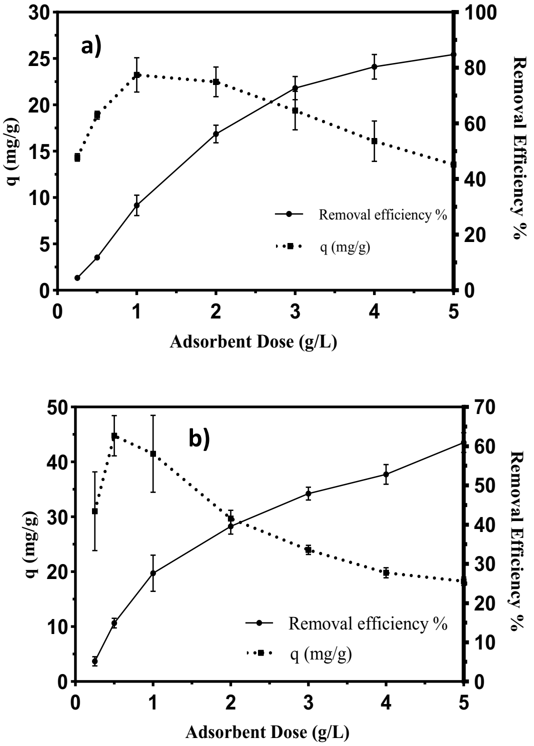

Figure 4. Influence of biosorbent dosage on tetracycline (TC) (a) and ciprofloxacin (CIP) (b) adsorption onto date palm fiber. Initial TC concentration: 80 mg L^{-1}, initial CIP concentration: 150 mg L^{-1}, temperature: 298 K, contact time: 3 h.

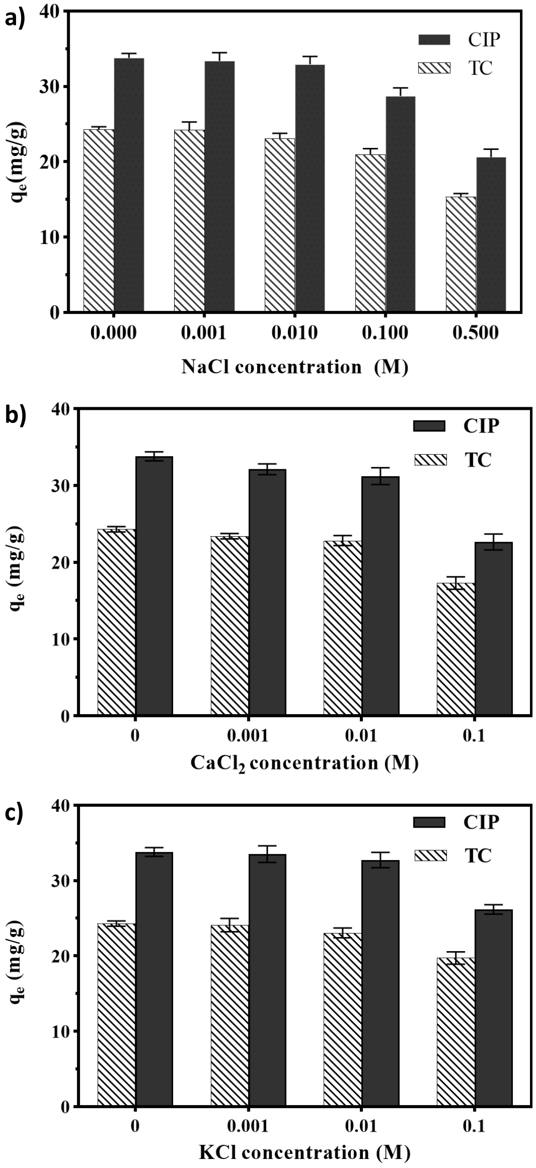

Figure 5. Effect of NaCl (a), $CaCl_2$ (b), and KCl (c) concentrations on the adsorption of tetracycline (TC) and ciprofloxacin (CIP) onto DP fiber. Initial TC concentration: 80 mg L^{-1}, initial CIP concentration: 150 mg L^{-1}, temperature: 298 K.

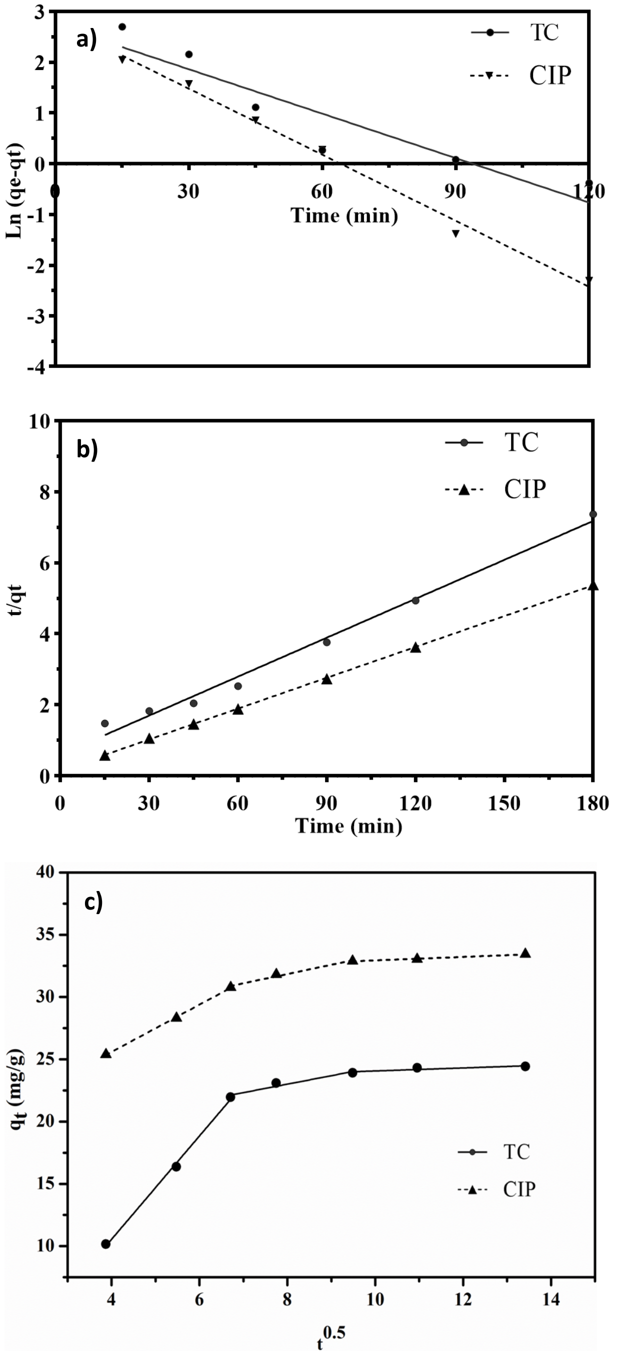

Figure 6. Pseudo-first-order (a), pseudo-second-order (b), and Weber-Morris linear plots used to describe the kinetics of tetracycline (TC) and ciprofloxacin (CIP) adsorption onto date palm fiber. Initial TC concentration: 80 mg L^{-1}, initial CIP concentration: 150 mg L^{-1}, temperature: 298 K.

and lower standard deviation of residuals (*Sy.x*) of the pseudo-second-order model indicate better fittings than the pseudo-first-order one. This implies that antibiotic biosorption was controlled by chemisorption or chemical interactions, involving sharing or exchange of electrons between adsorbent and adsorbate. An increase in *q* is then envisaged, which is directly related to the number of active sites present on surface [40].

The W-M model was also used to better understand the rate-controlling steps. Typically, when kinetic data exhibit multiple linear regions, adsorption is governed by multiple-step diffusion. If only intraparticle diffusion is involved, the plot of *q* versus the square root of time (Eq. (S11)) displays a straight line passing through the origin [35, 40]. As depicted in Fig. 6c, the plots exhibited a mult-linear pattern, suggesting the presence of two or more steps. The initial step, with steeper slope, indicates external or random adsorption, while in the subsequent curve regions intraparticle diffusion was the likely rate-limiting step. In the final equilibrium step, the intraparticle diffusion rate gradually slowed down due to (a) reduction in pore size,

Table 1. Parameters of kinetic models tested in this study to describe tetracycline and ciprofloxacin adsorption onto date palm fiber.

Model	Parameter	Adsorbate	
		Tetracycline	Ciprofloxacin
Pseudo-first-order	k_1 [min^{-1}]	0.029	0.052
	R^2 [–]	0.866	0.996
	Sy.x [–]	0.502	0.154
Pseudo-second-order	k_2 [g mg^{-1}min^{-1}]	0.0021	0.0063
	R^2 [–]	0.989	0.999
	Sy.x [–]	0.24	0.02
Weber-Morris	k_{i1} [mg g^{-1} min$^{-0.5}$]	4.15	1.89
	C_{i1} [mg g^{-1}]	–6.06	18
	R_1^2 [–]	0.998	0.992
	Sy.x [–]	0.38	0.11
	k_{i2} [mg g^{-1} min$^{-0.5}$]	0.68	0.744
	C_{i2} [mg g^{-1}]	17.56	25.89
	R_2^2 [–]	0.945	0.981
	Sy.x [–]	0.326	0.205
	k_{i3} [mg g^{-1} min$^{-0.5}$]	0.121	0.14
	C_{i3} [mg g^{-1}]	22.86	31.54
	R_3^2 [–]	0.799	0.989
	Sy.x [–]	0.17	0.04

(b) increase in electrostatic repulsion, and (c) decrease in antibiotic concentration.

As shown in Tab. 1, k_i and C_i values in these steps decreased and increased over time, respectively, throughout adsorption. Whereas an intercept increase indicates a greater contribution of surface sorption in the rate-controlling step [40], negative C_i values imply the absence of any boundary layer effect on the adsorption rate [41].

Biosorption data were then fitted with the Langmuir, Freundlich, Temkin, and D-R isotherms (Fig. 7), whose estimated parameters are given in Tab. 2. The Langmuir model accurately described TC adsorption with higher R^2 value compared to other isotherms, which suggests homogeneous adsorbent surface with a limited number of identical and independent adsorption sites, under equilibrium and forming a monolayer [42]. Oppositely, the D-R isotherm showed the highest R^2 value for CIP, indicating that energy distribution and DP surface characteristics played a significant role in the adsorption.

The E value below 8 kJ mol^{-1} suggests that physical adsorption likely contributed to the process [43]. Additionally, the Temkin isotherm, which assumes linear decrease in the adsorption heat and uniform distribution of binding energies across the surface, was employed to explain the interactions between DP fiber and antibiotics. The positive b_T values indicate exothermic TC and CIP adsorption as the adsorption heat decreases linearly with increasing recovery rate [42, 44]. However, this model alone does not provide sufficient information to determine the endothermic or exothermic nature of adsorption. A thermodynamic study was then conducted to further investigate this issue, which confirmed the endothermicity of the process (Supporting Information, Sect. S3).

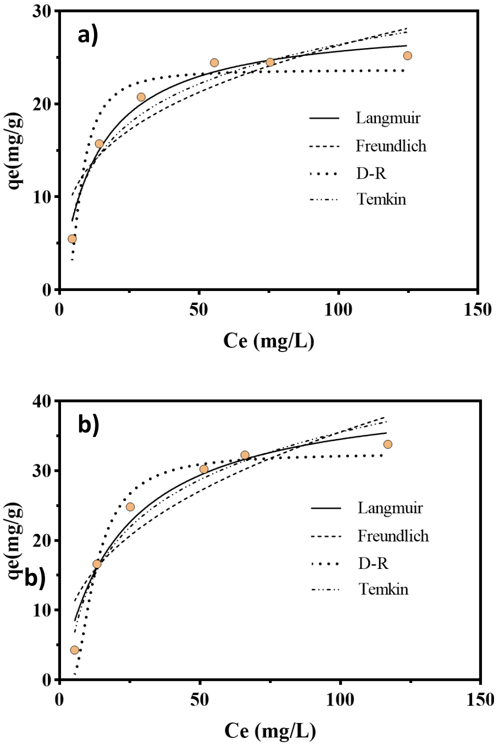

Figure 7. Isotherms of tetracycline (a) and ciprofloxacin (b) adsorption onto DP fiber. Temperature: 298 K, contact time: 2 h.

The maximum biosorption capacities (q_m) were shown to be 29.16 mg g^{-1} using the Langmuir model for TC and 32.54 mg g^{-1} using the D-R model for CIP. To our knowledge, no previous study was published on TC and CIP biosorption onto DP; nonetheless, these q_m values are close to those reported for other materials used to adsorb these antibiotics [45–47].

4 Conclusions and Future Prospects

In the current study, the factors influencing TC and CIP removal using raw DP fiber as an adsorbent were investigated in batch experiments. This agricultural by-product showed high efficacy in the adsorption of both antibiotics, being able to remove more than 84 % of TC and 66 % of CIP at concentrations of 80 and 150 mg L^{-1}, respectively. In both cases, reaction kinetics was satisfactorily described by the pseudo-second-order model, while biosorption isotherms demonstrated conformity with the Langmuir model for TC and the D-R model for CIP. Adsorption of targeted antibiotics and others onto DP fiber modified in different ways will be investigated in future work either using them alone or in combination.

Table 2. Parameters of the isotherm models tested in this study to describe tetracycline and ciprofloxacin adsorption onto date palm fiber.

Model	Parameter	Adsorbate	
		Tetracycline	Ciprofloxacin
Langmuir	q_m [mg g^{-1}]	29.16	41.47
	K_L [L mg^{-1}]	0.075	0.049
	R^2 [–]	0.977	0.953
	Sy.x [–]	1.292	2.8
Freundlich	n [–]	0.307	0.384
	K_F [mg$^{1-1/n}$L$^{1/n}$g^{-1}]	6.405	6.058
	R^2 [–]	0.845	0.837
	Sy.x [–]	3.376	5.13
D-R	q_s [mg g^{-1}]	23.68	32.54
	B [mol^2 kJ^{-2}]	8.176	20.24
	E [kJ mol^{-1}]	0.247	0.157
	R^2 [–]	0.923	0.975
	Sy.x	2.371	1.99
Temkin	b_T [J mol^{-1}]	405.56	253.72
	A_T [L mol^{-1}]	0.751	0.382
	R^2 [–]	0.939	0.944
	Sy.x [–]	2.119	3.004

Supporting Information

Supporting Information for this article can be found under DOI: https://doi.org/10.1002/ceat.202300193. This section includes additional references to primary literature relevant for this research [48–51].

Acknowledgment

This research has been funded by the Research Deanship of University of Ha'il, Saudi Arabia through project number RG-21014.

The authors have declared no conflict of interest.

Symbols used

A_T	[L mol^{-1}]	equilibrium binding constant
B	[mol^2 kJ^{-2}]	parameter depending on the free energy of adsorption
b_T	[J mol^{-1}]	adsorption heat
C_0	[mg L^{-1}]	initial antibiotic concentration
C_e	[mg L^{-1}]	antibiotic concentration at equilibrium
C_i	[mg g^{-1}]	intercept in Weber-Morris model
E	[kJ mol^{-1}]	average adsorption free energy
$\Delta G°$	[kJ mol^{-1}]	standard Gibbs free energy change
$\Delta H°$	[kJ mol^{-1}]	standard enthalpy change
K_D	[L g^{-1}]	distribution coefficient
K_F	[mg$^{1-1/n}$L$^{1/n}$g^{-1}]	adsorption constant of Freundlich equation
k_i	[mg g^{-1}min$^{-0.5}$]	intraparticle diffusion rate constant
K_L	[L mg^{-1}]	adsorption constant of Langmuir equation
m	[g]	weight of dried biosorbent
n	[–]	biosorption intensity
q	[mg g^{-1}]	adsorption capacity
q_e	[mg g^{-1}]	equilibrium adsorption capacity
q_m	[mg g^{-1}]	maximum biosorption capacity
q_s	[mg g^{-1}]	maximum adsorption capacity in D-R isotherm
R	[J mol^{-1}K^{-1}]	ideal gas constant
$\Delta S°$	[J mol^{-1}K^{-1}]	standard entropy change
T	[K]	temperature
V	[L]	solution volume
Y	[%]	removal efficiency

Greek letter

ε	[kJ mol^{-1}]	adsorption potential

References

[1] B. Sarker, K. N. Keya, F. I. Mahir, K. M. Nahiun, S. Shahida, R. A. Khan, *Guigoz Sci. Rev.* **2021**, *7 (3)*, 32–41. DOI: https://doi.org/10.32861/sr.73.32.41

[2] A. Hossain, M. Habibullah-Al-Mamun, I. Nagano, S. Masunaga, D. Kitazawa, H. Matsuda, *Environ. Sci. Pollut. Res.* **2022**, *29 (8)*, 11054–11075. DOI: https://doi.org/10.1007/s11356-021-17825-4

[3] N. Azian, A. Mohd, A. Ahmad, B. H. Hameed, A. Taufik, M. Din, *Environ. Sci. Pollut. Res.*, in press. DOI: https://doi.org/10.1007/s11356-022-19829-0

[4] I. N. Lykov, V. S. Volodkin, *IOP Conf. Ser.: Earth Environ. Sci.* **2021**, *677 (5)*, 52044. DOI: https://doi.org/10.1088/1755-1315/677/5/052044

[5] P. R. Rout, T. C. Zhang, P. Bhunia, R. Y. Surampalli, *Sci. Total Environ.* **2021**, *753*, 141990. DOI: https://doi.org/10.1016/j.scitotenv.2020.141990

[6] O. Alegbeleye, O. B. Daramola, A. T. Adetunji, O. T. Ore, Y. J. Ayantunji, R. K. Omole, D. Ajagbe, S. O. Adekoya, *Environ. Sci. Pollut. Res.* **2022**, *29 (38)*, 56948–57020. DOI: https://doi.org/10.1007/s11356-022-21252-4

[7] A. I. Shah, M. U. Din Dar, R. A. Bhat, J. P. Singh, K. Singh, S. A. Bhat, *Ecol. Eng.* **2020**, *152*, 105882. DOI: https://doi.org/10.1016/j.ecoleng.2020.105882

[8] H. Ding, Y. Wu, B. Zou, Q. Lou, W. Zhang, J. Zhong, L. Lu, G. Dai, *J. Hazard. Mater.* **2016**, *307*, 350–358. DOI: https://doi.org/10.1016/j.jhazmat.2015.12.062

[9] D. Mangla, Annu, A. Sharma, S. Ikram, *J. Hazard. Mater.* **2022**, *425*, 127946. DOI: https://doi.org/10.1016/j.jhazmat.2021.127946

[10] N. Cheng, B. Wang, P. Wu, X. Lee, Y. Xing, M. Chen, B. Gao, *Environ. Pollut.* **2021**, *273*, 116448. DOI: https://doi.org/10.1016/j.envpol.2021.116448

[11] M. Varsha, P. Senthil Kumar, B. Senthil Rathi, *Chemosphere* **2022**, *287*, 132270. DOI: https://doi.org/10.1016/j.chemosphere.2021.132270

[12] S. Uçar, M. Erdem, T. Tay, S. Karagöz, *Appl. Surf. Sci.* **2009**, *255 (21)*, 8890–8896. DOI: https://doi.org/10.1016/j.apsusc.2009.06.080

[13] S. Husien, R. M. El-taweel, A. I. Salim, I. S. Fahim, L. A. Said, A. G. Radwan, *Curr. Res. Green Sustainable Chem.* **2022**, *5*, 100325. DOI: https://doi.org/10.1016/j.crgsc.2022.100325

[14] S. Al Arni, M. Elwaheidi, A. Converti, M. Benaissa, A. A. M. Salih, S. Ghareba, N. Abbas, *ChemBioEng Rev.* **2023**, *10 (1)*, 55–64. DOI: https://doi.org/10.1002/cben.202200008

[15] A. Othmani, S. Magdouli, P. Senthil Kumar, A. Kapoor, P. V. Chellam, Ö. Gökkuş, *Environ. Res.* **2022**, *204*, 111916. DOI: https://doi.org/10.1016/j.envres.2021.111916

[16] B. Ravindran, M. Feuchter, R. Schledjewski, *J. Compos. Sci.* **2023**, *7 (3)*, 122. DOI: https://doi.org/10.3390/jcs7030122

[17] P. Logam, A. Kumbahan, *Sains Malays.* **2018**, *47 (1)*, 35–49. DOI: https://doi.org/10.17576/jsm-2018-4701-05

[18] E. Pehlivan, T. Altun, S. Cetin, M. Iqbal Bhanger, *J. Hazard. Mater.* **2009**, *167 (1)*, 1203–1208. DOI: https://doi.org/10.1016/j.jhazmat.2009.01.126

[19] M. T. Amin, A. A. Alazba, M. N. Amin, *Pol. J. Environ. Stud.* **2017**, *26 (2)*, 543–557. DOI: https://doi.org/10.15244/pjoes/66963

[20] K. K. Wong, C. K. Lee, K. S. Low, M. J. Haron, *Process Biochem.* **2003**, *39 (4)*, 437–445. DOI: https://doi.org/10.1016/S0032-9592(03)00094-3

[21] M. F. Hossain, *Agric., Ecosyst. Environ.* **2006**, *113 (1–4)*, 1–16. DOI: https://doi.org/10.1016/j.agee.2005.08.034

[22] K. Riahi, A. Ben Mammou, B. Ben Thayer, *J. Hazard. Mater.* **2009**, *161 (2)*, 608–613. DOI: https://doi.org/10.1016/j.jhazmat.2008.04.013

[23] M. Gouamid, M. R. Ouahrani, M. B. Bensaci, *Energy Procedia* **2013**, *36*, 898–907. DOI: https://doi.org/10.1016/j.egypro.2013.07.103

[24] M. Liu, Y. Zhang, M. Yang, Z. Tian, L. Ren, S. Zhang, *Environ. Sci. Technol.* **2012**, *46 (14)*, 7551–7557. DOI: https://doi.org/10.1021/es301145m

[25] R. S. Lamarca, R. Faria, M. Zanoni, M. Nalin, P. Lima Gomes, Y. Messaddeq, *RSC Adv.* **2020**, *10*, 1838–1847. DOI: https://doi.org/10.1039/c9ra09083e

[26] S. K. Mondal, A. K. Saha, A. Sinha, *J. Cleaner Prod.* **2018**, *171*, 1203–1214. DOI: https://doi.org/10.1016/j.jclepro.2017.10.091

[27] W. Tan, S. Lu, F. Liu, X. Feng, J.-Z. He, L. Koopal, *Soil Sci.* **2008**, *173 (4)*, 277–286. DOI: https://doi.org/10.1097/SS.0b013e31816d1f12

[28] W. Xiang, Y. Wan, X. Zhang, Z. Tan, T. Xia, Y. Zheng, B. Gao, *Chemosphere* **2020**, *255*, 127057. DOI: https://doi.org/10.1016/j.chemosphere.2020.127057

[29] S. Xing, W. Li, B. Liu, Y. Wu, Y. Gao, *Chem. Eng. J.* **2020**, *382*, 122837. DOI: https://doi.org/10.1016/j.cej.2019.122837

[30] Y. Li, S. Wang, Y. Zhang, R. Han, W. Wei, *J. Mol. Liq.* **2017**, *247*, 171–181. DOI: https://doi.org/10.1016/j.molliq.2017.09.110

[31] J. Zhao, Y. Dai, *Environ. Sci. Pollut. Res.* **2022**, *29 (6)*, 9142–9152. DOI: https://doi.org/10.1007/s11356-021-16329-5

[32] V. Rizzi et al., *Sci. Total Environ.* **2019**, *693*, 103620. DOI: https://doi.org/10.1016/j.scitotenv.2019.133620

[33] T. Ahamad, M. Naushad, T. Al-Shahrani, N. Al-hokbany, S. M. Alshehri, *Int. J. Biol. Macromol.* **2020**, *147*, 258–267. DOI: https://doi.org/10.1016/j.ijbiomac.2020.01.025

[34] S. A. C. Carabineiro, T. Thavorn-Amornsri, M. F. R. Pereira, J. L. Figueiredo, *Water Res.* **2011**, *45 (15)*, 4583–4591. DOI: https://doi.org/10.1016/j.watres.2011.06.008

[35] D. Balarak, A. H. Mahvi, M. J. Shim, S. M. Lee, *Desalin. Water Treat.* **2021**, *212*, 390–400. DOI: https://doi.org/10.5004/dwt.2021.26603

[36] M. Z. Afzal, X. F. Sun, J. Liu, C. Song, S. G. Wang, A. Javed, *Sci. Total Environ.* **2018**, *639*, 560–569. DOI: https://doi.org/10.1016/j.scitotenv.2018.05.129

[37] H. Wu, H. Xie, G. He, Y. Guan, Y. Zhang, *Appl. Clay Sci.* **2016**, *119*, 161–169. DOI: https://doi.org/10.1016/j.clay.2015.08.001

[38] Z. W. Zeng, X. F. Tan, Y. G. Liu, S. R. Tian, G. M. Zeng, L. H. Jiang, S. B. Liu, J. Li, N. Liu, Z. H. Yin, *Front. Chem.* **2018**, *6*, 80. DOI: https://doi.org/10.3389/fchem.2018.00080

[39] C. Peiris, S. R. Gunatilake, T. E. Mlsna, D. Mohan, M. Vithanage, *Bioresour. Technol.* **2017**, *246*, 150–159. DOI: https://doi.org/10.1016/j.biortech.2017.07.150

[40] D. Balarak, M. Baniasadi, S. Lee, M. Shim, *Desalin. Water Treat.* **2021**, *218*, 444–453. DOI: https://doi.org/10.5004/dwt.2021.26986

[41] K. Z. Elwakeel, A. A. Atia, E. Guibal, *Bioresour. Technol.* **2014**, *160*, 107–114. DOI: https://doi.org/10.1016/j.biortech.2014.01.037

[42] F. Mostafapour, A. Mahvi, A. Khatibi, M. Khodadadi Saloot, N. Mohammadzadeh, D. Balarak, *Desalin. Water Treat.* **2022**, *265*, 103–113. DOI: https://doi.org/10.5004/dwt.2022.28627

[43] F. Mostafapour, M. Yılmaz, A. Mahvi, A. Younesi, F. Ganji, D. Balarak, *Desalin. Water Treat.* **2022**, *247*, 216–228. DOI: https://doi.org/10.5004/dwt.2022.27943

[44] A. Khatibi, M. Yılmaz, A. Mahvi, D. Balarak, S. Salehi, *Desalin. Water Treat.* **2022**, *271*, 48–57. DOI: https://doi.org/10.5004/dwt.2022.28812

[45] Q. Zaib, U. Ryenchindorj, A. S. Putra, D. Kyung, H.-S. Park, *Environ. Sci. Pollut. Res.* **2023**, *30*, 4972–4985. DOI: https://doi.org/10.1007/s11356-022-22476-0

[46] T. Ahamad, Ruksana, A. A. Chaudhary, M. Naushad, S. M. Alshehri, *Int. J. Biol. Macromol.* **2019**, *134*, 180–188. DOI: https://doi.org/10.1016/j.ijbiomac.2019.04.204

[47] H. R. Pouretedal, N. Sadegh, *J. Water Process Eng.* **2014**, *1*, 64–73. DOI: https://doi.org/10.1016/j.jwpe.2014.03.006

[48] M. T. Amin, A. A. Alazba, M. Shafiq, *Desalin. Water Treat.* **2016**, *57 (47)*, 22454–22466. DOI: https://doi.org/10.1080/19443994.2015.1131635

[49] A. Chandrasekaran, C. Patra, S. Narayanasamy, S. Subbiah, *Environ. Res.* **2020**, *188*, 109825. DOI: https://doi.org/10.1016/j.envres.2020.109825

[50] M. Simić, J. Petrović, T. Šoštarić, M. Ercegović, J. Milojković, Z. Lopičić, M. Kojić, *Processes* **2022**, *10 (10)*, 1957. DOI: https://doi.org/10.3390/pr10101957

[51] A. A. Mohammed, T. J. Al-Musawi, S. L. Kareem, M. Zarrabi, A. M. Al-Ma'abreh, *Arabian J. Chem.* **2020**, *13 (3)*, 4629–4643. DOI: https://doi.org/10.1016/j.arabjc.2019.10.010